Experimental determination of 3D Green's function in composite plates for defect imaging using guided waves

Andrii Kulakovskyi, Olivier Mesnil, Bastien Chapuis, Oscar d'Almeida, Alain Lhémery

9th European Workshop on Structural Health Monitoring
July 10-13, 2018, Manchester, United Kingdom

Experimental determination of 3D Green's function in composite plates for defect imaging using guided waves

Andrii Kulakovskyi[1,2], Olivier Mesnil[2], Bastien Chapuis[2], Oscar d'Almeida[1] and Alain Lhémery[2]
1 SAFRAN Tech, France
2 CEA LIST, France

Abstract

Carbon fibre reinforced polymer (CFRP) plates and honeycomb composite sandwich structures (HCSS) are widely used in the aerospace industry as they exhibit excellent mechanical properties. Nevertheless, defects such as face sheet delamination or core-sheet debonding can appear due to impact forces or thermomechanical aging and may degrade these properties. Structural Health Monitoring (SHM) system, based on the use of Guided elastic Waves (GWs), is considered as a promising solution for such defect detection. The GWs propagate over long distances while being sensitive to structural inhomogeneities. Our system prototype relies on a sparse grid of piezo-electric transducers distributed over the structure, used for both GW actuating and sensing. Defect imaging is performed by means of a correlation-based algorithm named Excitelet. It is based on the calculation of correlation coefficients between theoretical and experimental GW signals for each pixel of cartography that represents the structure. The 3D Green's function is required in order to reconstruct theoretical signal for each pixel of the cartography grid. In our approach, it is experimentally determined from the 3D wavefield in pristine CFRP plate and HCSS. Defect imaging is then performed in both structures using abovementioned 3D Green's functions. Results are illustrated, conclusions are drawn.

1. Introduction

In the past years, the use of composite materials in the aerospace industry has considerably increased. Such rapid growth is mainly due to their excellent mechanical properties and a relatively light mass of the composite structures. Nevertheless, defects such as plies delamination, debonding or corrosion may appear due to thermomechanical aging or impact forces and can degrade these properties. Aforesaid structural flaws often occur within the structure being barely detectable on the surface to the naked eye [1]. They can expand internally to the large volumes up to the structure collapse. Moreover, such composite structures are often hardly accessible to the maintenance team performing regular non-destructive examination. Composite structure manufacturers introduce a safety margin design to resist accidental impacts and structure aging. It leads to the additional weight of the structure and consequent economic shortcomings.

Aforementioned reasons became a driving force for the development of structural health monitoring system to provide an accurate localization and quantification of damages in composite structures while being robust to the environmental effects such as temperature and humidity variations, accumulated strains, etc. Such a SHM system can potentially

replace scheduled maintenance, reduce safety margin design, hence introduce significant economic benefit.

Guided elastic waves have been proven effective for structure inspection as they can propagate over large distances while being sensitive to structural defects. Among other SHM methods, GWs can be easily actuated and sensed by a network of piezo-electric transducers attached to the surface. Defect imaging algorithm process these signals in order to compute cartography of the structure, which is an image that represents the healthiness of the inspected specimen [1, 2].

In the current work, the defect imaging is performed by means of a correlation-based algorithm named Excitelet. It computes a correlation coefficient between theoretical and experimental GW signals for each pixel of cartography. The 3D Green's function (3DGF) of the structure is required to obtain the theoretical signal [2]. For the plate-like structures, the 3DGF of each propagating mode can be obtained via various modeling tools. However, it may be difficult to compute them for the real complex shape structures. Therefore, a method for experimental determination of 3DGF is required to overcome an additional complexity introduced by the presence of stiffeners, joints, etc.

This paper is organized as follows. Firstly, a brief review of defect imaging algorithms is presented. After that, our approach for 3DGF determination is described. Defect imaging results using experimental 3DGF are then presented and conclusions are drawn.

2. Guided waves imaging methodology

The Guided Wave Imaging (GWI) is one of the most effective approaches to evaluate 'healthiness' of the structure. It implies a cartography computation for the region of interest of the studied specimen, where each pixel is mapped to the corresponding segment of the structure. A flaw presence, localization, and severity are deduced from analyzing the spatial intensity distribution on the cartography.

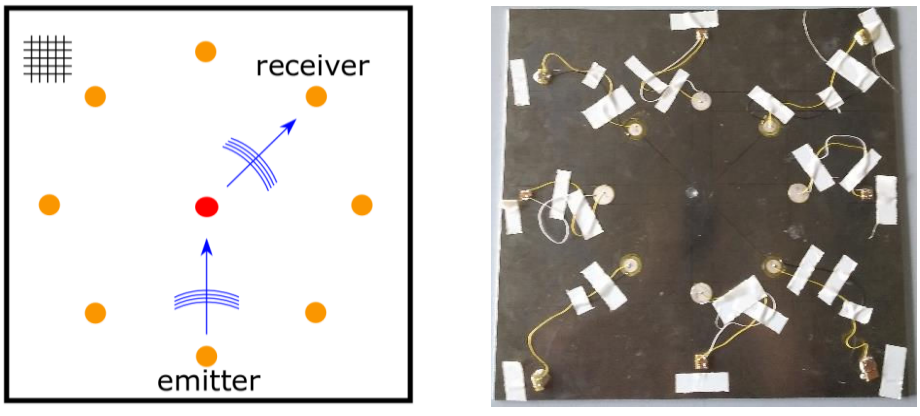

(a) (b)

Figure 1: Illustration of GWI methodology for defect cartography computation. (a) Cartography representing the studied specimen; yellow and red circles denote PZTs and flaw locations respectively, and blue arrows correspond to GWs propagating in the structure. (b) Photo of the aluminum plate equipped with the sparse grid of the PZT transducers; a flat bottom hole serves as a structural defect.

A schematic of the GWI procedure is represented in Figure 1. The grid of pixels discretizes the region of interest of the studied specimen. In the study presented, we use a demanding baseline algorithm, named Excitelet, which attributes a global Damage Index (DI) value to each pixel. Exploiting the GW propagation specifications, it processes residual signals (defined as the difference between pristine and damaged states of the structure) that are measured by each pair of piezo-electric transducers distributed over the structure. It is also assumed that the wavelength of the excited GW is of the same order of magnitude as the defect size to observe GW's diffraction effects. Therefore, the residual signals contain 'echoes' coming from the defect.

Aforementioned global DI value (1) is obtained as the sum of the local DI_j (2) values computed for each PZT j[th] pair [2, 3]. The latter is expressed via modulus of a correlation coefficient between the experimental residual and theoretical signal, which is computed assuming the presence of one punctual isotropic scatterer at the considered location. It is the GW packet that is propagated from the emitter to the point of interest and from latter one to the receiver .

$$DI(x_i, y_i) = \sum_j DI_j(x_i, y_i) \tag{1}$$

$$DI_j(x_i, y_i) = \left| \frac{\int_{t_0}^{t_{max}} S^{exp}_{emit_j \to rec_j}(t)\, S^{theor}_{emit_j \to rec_j}(t) dt}{\sqrt{\int_{t_0}^{t_{max}} \left(S^{exp}_{emit_j \to rec_j}(t)\right)^2 dt \int_{t_0}^{t_{max}} \left(S^{theor}_{emit_j \to rec_j}(t)\right)^2 dt}} \right|, \tag{2}$$

where $DI(x_i, y_i)$ denotes damage index value for a (x_i, y_i) pixel, $S^{exp}_{emit_j \to rec_j}(t)$ denotes the experimental residual signal and $S^{theor}_{emit_j \to rec_j}(t)$ denotes the theoretical signal for the corresponding PZT pair. The theoretical signal can be calculated as a convolution of an excitation function with the Green's function (3) that describes the GW propagation in the structure of interest:

$$S^{theor}_{emit \to rec}(r, \alpha, t) = u(t) * G_{emit \to obs}(r_1, \alpha, t) * G_{obs \to rec}(r_2, \alpha, t), \tag{3}$$

where $u(t)$ denotes excitation function, $G(r, \alpha, t)$ is the Green's function, r_1 and r_2 denote the distances from an emitter to an observation point and to a receiver respectively and α denotes angle on GWs propagation.

3. Experimental determination of 3D Green's function

The 3DGFs are necessary for the theoretical signal computation. For the simple shape structures (i.e., plates, pipes, rails, etc.), they can be computed via analytical modeling methods such as SAFE or GMM [4, 5]. However, real-life structures are often equipped with stiffeners or joints, which introduce additional complexity. They modify the 3DGF of each propagating mode, so the analytical determination is no longer possible. On the other hand, classical finite element modeling method can be used to model structures of any complexity but it requires a tedious meshing procedure, significant computation time and, even though, it does not provide separate solutions for each propagating mode.

In this section, an experimental approach for 3DGF determination in the composite plate is discussed. This method can be decomposed into the following steps:

- Guided wavefield acquisition
- Experimental determination of the 3DGF

Each step is developed and discussed in the following sub-sections.

3.1 GW wavefield acquisition

The first step consists of the GW wavefield acquisition over the region of interest. This region is usually quite large as the extracted 3DGF will be used for defect imaging. The standard Scanning Laser Doppler Vibrometer (SLDV) is used to measure the GWs propagation [6]. This procedure is highly time-consuming as the dense grid of measurement points is required. In order to overcome this issue, we addressed to the Gaussian Process Regressor (GPR) to build a non-parametric model of the 3D wavefield.

This wavefield model is obtained thanks to transfer learning. In this framework, GPR seeks to simultaneously learn time steps of the GW signals at available coordinates by estimating the correlation function between them and translating previously acquired information to the unseen point of the wavefield. In other words, we perform spatially sparse GW measurements, and GPR reconstructs missing signals. The GPR model also provides uncertainty information that can be used to derive models precision, see Figure 2.

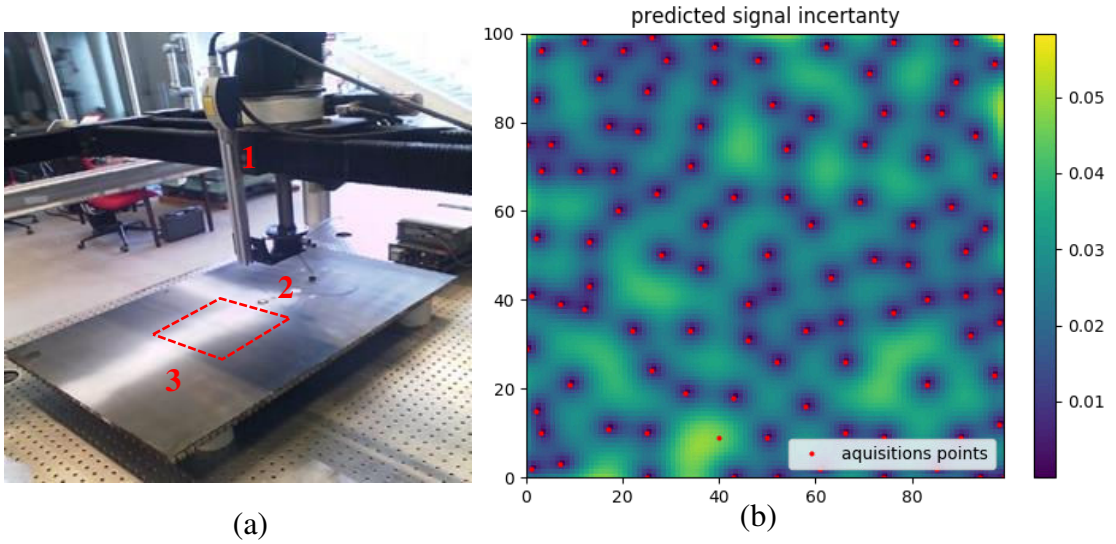

Figure 2: (a) Photo of laser vibrometer based setup used for GW wavefield acquisition: 1 – SLDV , 2 – PZT, 3 – user-defined area of measurements. (b) The uncertainty map obtained from the GPR model of the 3D wavefield 100x100 mm.

The Matern kernel has been chosen as a covariance function for GPR, as it is a combination of Gamma and Bessel functions, which, to the knowledge of authors, is a

good approach to reconstruct a 3D wavefield. For example, a region of interest $100x100$ pixels, shown in Figure 2, can be reconstructed with 350 acquisition points.

3.2 Experimental determination of 3D *Green's function*

The second step consists of the application of a spectral filter to each direction of GW propagation. Directional GW time series (i.e., b-scan) are obtained thanks to the GPR model, and the corresponding dispersion curves are obtained via two dimensional Fourier transform applied to the b-scan. The part of the $(f - k)$ distribution corresponding to the GW reflections and negative frequencies is zeroed, so only incident waves are preserved. The filtered spectrum is transformed back to space-time domain via inverse 2D-FFT [7], see Figure 3.

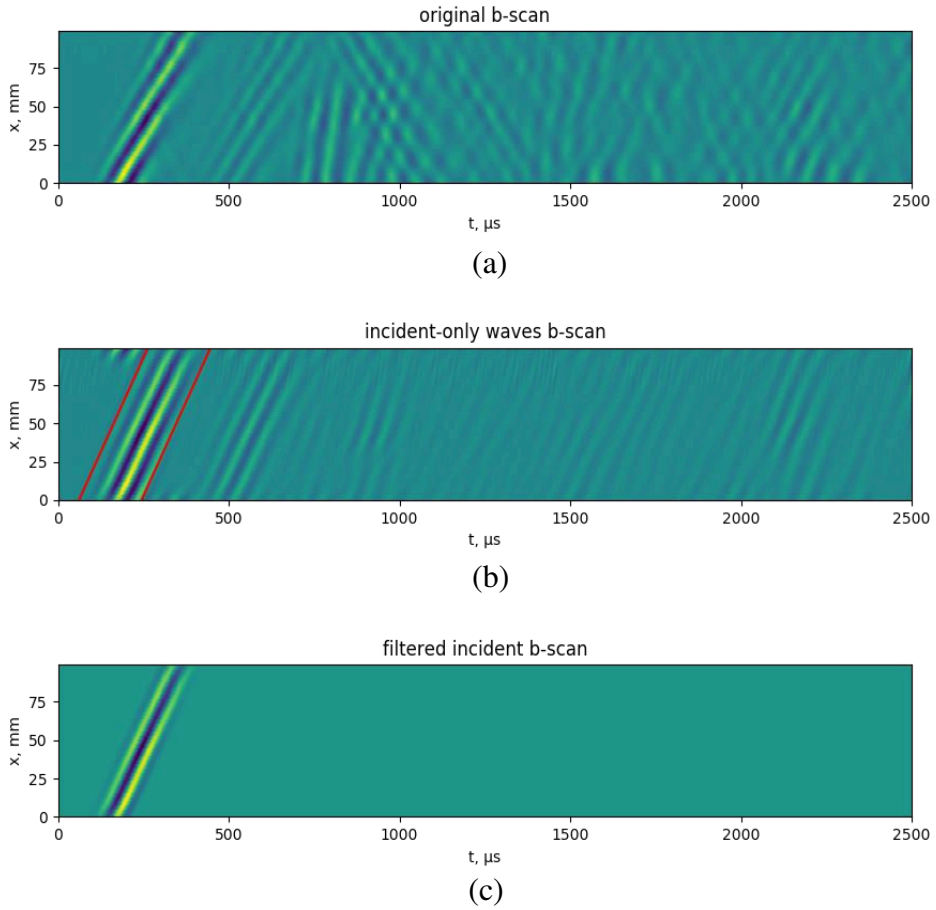

Figure 3: (a) b-scan reconstructed from the GPR model, (b) the filtered incident waves and reflections from the opposite side of the plate, (c) first packet extracted from the filtered b-scan.

Once only incident waves are present in the b-scan the first propagated packet corresponding to the mode m has to be extracted. The excitation frequency and PZT size have to be selected in such a way that the modes envelopes do not overlap. Boundaries of the first propagated packet of the mode m are obtained through the calculation of the gradient sign change while moving to the left and to the right from a maximum of the corresponding envelope, see Figure 4.

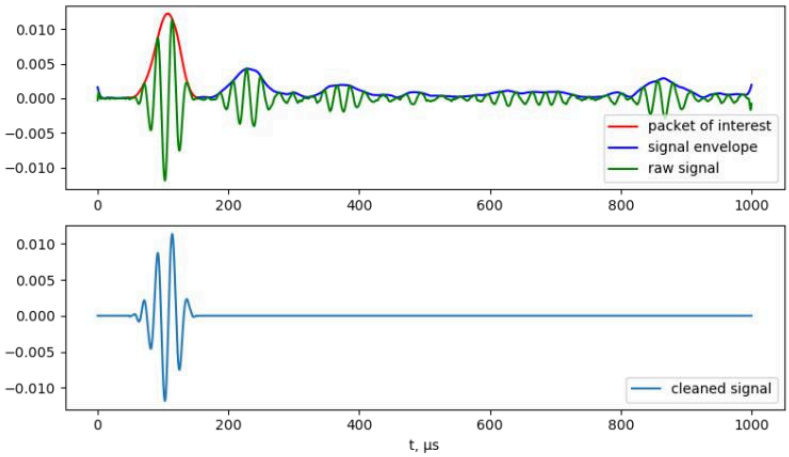

Figure 4: Filtering procedure for the first propagated packet identification that corresponds to the mode of interest.

As soon as the first propagated packet of the mode m is extracted, the 3D Green's function can be obtained as:

$$G(r,w) = \frac{U(r,w) * P(0,w)^*}{|P(0,w)^*|}, \quad (4)$$

where $U(r,w)$ is the filtered packet of the mode m propagated on the distance r at the w circular frequency and $P(0,w)$ represents the excitation function. This procedure is iteratively performed for each signal over the region of interest in order to experimentally determine the 3D Green's functions for the A_0 mode.

4. Defect imaging results using experimental 3D Green functions

Two composite structures are selected in this study. The first one is a layered CFRP plate (1000 mm x 600 mm) consisting of 21 plies, each 0.275mm thick. The second one is a HCSS 22.5 mm thick. The honeycomb core cell is 9.525 mm in diameter and 18.5 mm in height. Its bottom skin consists of four CFRP plies and one E-glass ply while the top skin consists of three CFRP plies and one E-glass. The 3DGFs are determined at 40 kHz and 15 kHz central frequencies for CFRP and HCSS respectively and are shown in Figure 5.

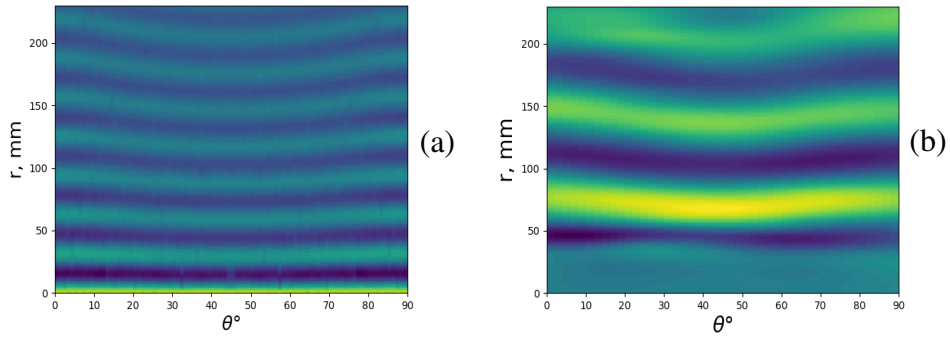

Figure 5: Real part of the 3D Green's function for (a) CFRP plate at 40 kHz and (b) HCSS at 15 kHz. There is a blind zone of 40 mm from the origin in 3DGF in HCSS as this region was not accessible during the wavefield acquisition.

The experimental 3DGFs are used in defect imaging algorithm Excitelet. The A_0 mode is selected for guided waves imaging in both structures. Sparse arrays of PZT transducers (each is 8 mm in diameter for CFR plate, and each is 20 mm in diameter for HCSS) are glued over the surface of both structures for GWs actuating and sensing. Hanning modulated three and two cycles bursts at 15 kHz and 40 kHz are selected as excitation functions for CFRP plate and HCSS inspection respectively. The defect imaging results are presented in Figure 6.

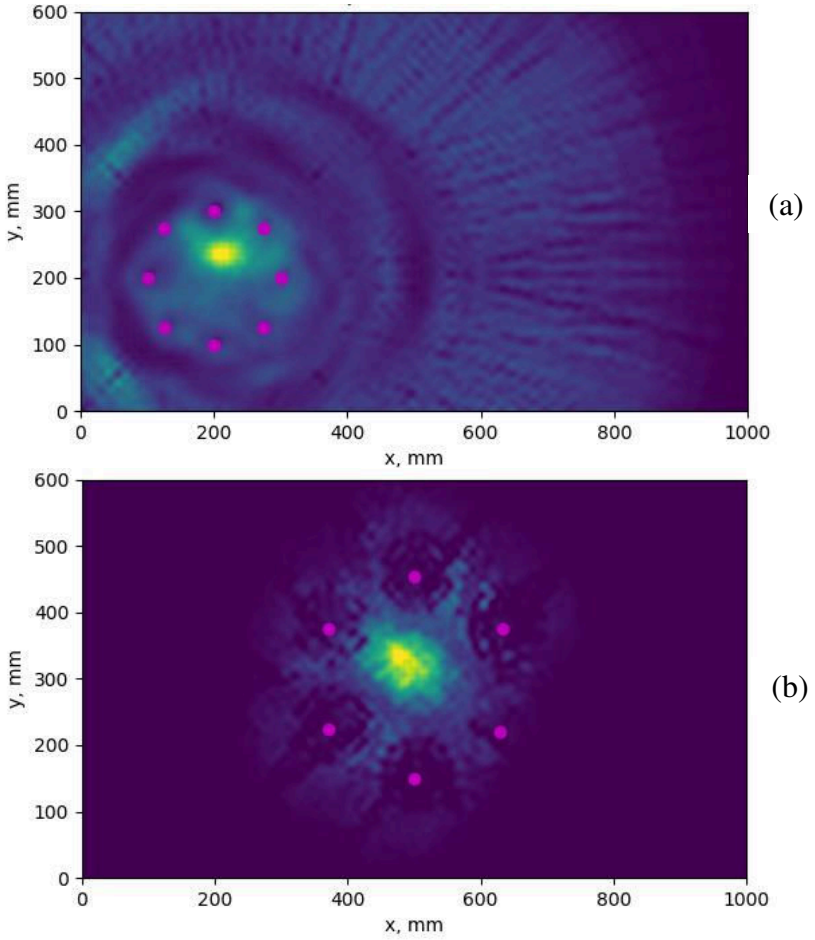

Figure 6: (a) Defect imaging in the (a) CFRP plate and (b) HCSS while the flaw presence is simulated by an attached mass.

The DI spatial intensity distribution on the cartography is related to the wavelength of the propagating guided mode. In the present study, the HCSS was inspected by A_0 mode at 15 kHz with the wavelength $\lambda_{A0}^{HCSS} = 63\ mm$, while the CFRP plate was monitored at 40 kHz with the same mode and the corresponding wavelength $\lambda_{A0}^{CFRP} = 32\ mm$. Defect imaging resolution is decreased by the fact of doubling the wavelength. Thus, to achieve higher resolution, it is necessary to inspect structures in a higher frequency range in order to decrease the wavelength of the chosen mode.

4. Conclusions

This paper reports on the experimental determination of the 3D Green's function in the CFRP plate and HCSS. They are used for the defect imaging in both structures. Cartographies of the corresponding structures are obtained by means of a correlation-based algorithm named Excitelet. It requires residual experimental and theoretical signals. In previous works, the theoretical signals were obtained via modelling methods. Here we demonstrated the possibility to experimentally determine the 3D Green's function. They were obtained from the filtered 3D guided wavefield measured by SLVD and then used for defect imaging in both CFRP plate and HCSS. The advantage of this approach is that it allows overcoming the difficulty of analytical computation of guided modes in complex real-life composite structures.

The presented deconvolution method was successfully applied for the low frequency range where the guided modes can be separated. For further studies, we will focus on more advanced methods for the 3D Green's function experimental determination, in order to cover larger frequency range, i.e. to reach smaller wavelengths of the inspecting modes.

References

1. Su Z., Ye L., Lu, Y. "Guided lamb waves for identification of damage in composite structures: a review." Journal of Sound and Vibration, 295(3-5):753-780, 2006.
2. Ostiguy P.-C., Masson P., Quaegebeur N. et Elkoun S. "Sensitivity of the Excitelet Imaging Algorithm on Material Properties for Isotropic Structures." Proceedings of the International Workshop in Structural Health Monitoring-USA, 2011.
3. Masson P., "Assessment of a novel imaging technique for commercial structural health monitoring and NDT systems." Proceedings of International Workshop Smart Materials, Structures & NDT in Aerospace-Canada, 2011.
4. Song F., Huang G. L., Hudson K., "Guided wave propagation in honeycomb sandwich structures using a piezoelectric actuator/sensor system." Journal of Smart Materials and Structures, 2009.
5. Velichko A., Wilcox P.,"Modeling the excitation of guided waves in generally anisotropic multilayered media." Journal of the Acoustical Society of America, 2007.
6. Sharma V., "Laser Doppler Vibrometer for Efficient Structural Health Monitoring." Ph.D. Thesis, Georgia Institute of Technology, 2008.
7. Alleyne D., Cawley P., "A two-dimensional Fourier transform method for the measurement of propagating multimode signals." Journal of the Acoustical Society of America, 1990.